

Cramer-Rao Lower Bound Analysis for OTFS and OFDM Modulation Systems

Bowen Wang, Jianchi Zhu, Xiaoming She, Peng Chen
China Telecom Research Institute
Beijing, China

Email: {wangbw2, zhujc, shexm, chenpeng11}@chinatelecom.cn

Abstract—The orthogonal time frequency space (OTFS) modulation as a promising signal representation attracts growing interest for integrated sensing and communication (ISAC), yet its merits over orthogonal frequency division multiplexing (OFDM) remain controversial. This paper devotes to a comprehensive comparison of OTFS and OFDM for sensing from the perspective of Cramér-Rao lower bounds (CRLB) analysis. To this end, we develop the cyclic prefix (CP)-Free and CP-added model for OFDM, while for OTFS, we consider the Zak transform based and the Two-Step conversion based models, respectively. Then we rephrase these four models into a unified matrix format to derive the CRLB of the delays and doppler shifts for multipath scenario. Numerical results demonstrate the superiority of OTFS modulation for sensing, and the effect of physical parameters for performance achievement.

Index Terms—orthogonal time frequency space (OTFS), integrated sensing and communication (ISAC), orthogonal frequency division multiplexing (OFDM), Cramér-Rao lower bounds (CRLB), Zak transform.

I. INTRODUCTION

The integrated sensing and communication (ISAC) has emerged as a key technology in 6G due to the capability of functioning both as radars and communication systems [1]. One of the most important topics of ISAC is the integrated waveform design.

The well-known Orthogonal Frequency Division Multiplexing (OFDM) has achieved great success in wireless communications and has been extensively studied for localization [2], [3]. However, its spectral efficiency suffers from inter-symbol interference (ISI) and inter-carrier interference (ICI). Besides, the ability of its channel characterization is limited by the uncertainty principle, which may cause a deficiency of sensing ability [4]. Recently, a new modulation scheme named orthogonal time frequency space (OTFS) was proposed, which multiplexes quadrature amplitude modulation symbols in the delay-Doppler (DD) representation, therefore holds promise for more accurate capture of the physics of the channel [5]. Motivated by its potentiality for ISAC, there emerge several research direct at OTFS based channel parameters estimation [6], [7]. However, it still remains for us to exhibit the fundamental limit of OTFS based parameters estimation, especially the comparative analysis with OFDM. The Cramér-Rao lower bound (CRLB) as a fundamental limit on the variance of any unbiased estimator in statistical inference theory, is commonly used as a benchmark to evaluate various estimation algorithms

and can be viewed as an effective criterion to guide practical algorithms design [8].

Our analysis encompasses four modem schemes. The original OFDM transmission does not contain cyclic prefixes (CP), which we refer to as CP-Free OFDM. In order to resist the inter-symbol interference and inter-carrier interference caused by multipath propagation and frequency offset, respectively, a more standard CP-OFDM modulation which add a CP in front of each symbol is used in practical applications. As for OTFS, in order to ensure compatibility with existing OFDM systems, most prior work consider a two-step conversion on the receiver side, where the received time-domain signal is firstly converted to the time-frequency domain using an OFDM demodulator, followed by post-processing of this time-frequency signal into DD domain [5]. Recently, studies show that the direct conversion of the received time-domain signal to the DD domain via the Zak transform, is also feasible [9]. The resulting expression for the sampled DD domain signal model is not the same as that obtained by the two-step conversion. We refer to an OTFS modulation based on the direct conversion as the ZAK OTFS_{\pm} and that based on the two-step conversion as the $\text{two-step OTFS}_{\pm}$. We devote to clarifying the sensing abilities of OTFS and OFDM by deriving the CRLB of parameter estimation under these four signal models.

The remainder of the paper is organized as follows. In Section II, we construct point-to-point transmission models for the four types of modem schemes and subsequently represented them as a formally unified matrix signal model. In section III, we derive the CRLB of delay and Doppler shift estimations for the four types of schemes. Numerical results are provided in section IV to demonstrate the superiority of Zak-OTFS and Two-Steps OTFS, as well as the degradation of CP-OFDM for sensing.

II. SIGNAL MODEL

We respectively consider the OFDM and OTFS systems with single antenna transceiver over time-varying multipath channels. The physical resource includes bandwidth $B = M\Delta f$ and time duration NT , where Δf and $T = 1/\Delta f$ denote the subcarrier spacing (SCS) and the symbol duration, respectively. In this section, we establish the input-output models for the two systems considering four cases including CP-Free OFDM, CP-OFDM, Zak-OTFS, and Two-Steps OTFS.

A. Point-to-Point CP-Free OFDM Transmission

OFDM as an efficient multi-carrier modulation converts high speed serial communication data into N parallel data streams, and modulates these data on M orthogonal subcarriers, the composite OFDM baseband signal is then the summation of all the subcarriers

$$f(t) = \sum_{m=0}^{M-1} \sum_{n=0}^{N-1} x[n, m] e^{j2\pi(f_c + m\Delta f)(t - nT)} g_{tx}(t - nT) \quad (1)$$

where f_c is the carrier frequency, $x[n, m]$ is the transmitted data on the m -th subcarrier of the n -th symbol duration. $g_{tx}(t)$ denotes the transmit pulse, and is set to be the rectangular window of duration T by default.

Consider a time-frequency varying channel, i.e., its behavior changes with respect to (w.r.t.) the time instant and the subcarrier frequency, which may be represented as a continuum of elements that simultaneously provide both a corresponding delay and Doppler shift

$$h(\tau, \nu) = \sum_{p=1}^P h_p \delta(\tau - \tau_p) \delta(\nu - \nu_p) \quad (2)$$

where $h(\tau, \nu)$ is the DD spread function, or interpreted as a continuum of nonmoving scintillating scatterers by the delay-spread functions which is the inverse Fourier transform of its spectrum and can be expressed as

$$\gamma(t, \tau) = \int h(\tau, \nu) e^{j2\pi\nu t} d\nu \quad (3)$$

then by ignoring the noise for the sake of simplicity, we can obtain the following input-output relationship as [10]

$$y'(t) = \int \gamma(t, \tau) f(t - \tau) d\tau = \sum_{p=1}^P h_p f(t - \tau_p) e^{j2\pi\nu_p t} \quad (4)$$

where h_p , τ_p , ν_p denote the channel gain, delay, and Doppler shift of the p -th path, respectively. By sampling $y'(t)$ every T/M seconds in each OFDM symbol, we obtain

$$\begin{aligned} y'_{n', m'} &= y'(t)|_{t=n'T + m'T/M} \\ &= \sum_{p=1}^P h_p \sum_{m=0}^{M-1} \sum_{n=0}^{N-1} x[n, m] e^{j2\pi m\Delta f((n' + \frac{m'}{M} - n)T - \tau_p)} \\ &\quad g_{tx}(n'T + \frac{m'T}{M} - nT - \tau_p) e^{j2\pi\nu_p(n'T + \frac{m'T}{M})} \\ &= \begin{cases} \sum_{p=1}^P h_p \sum_{m=0}^{M-1} x[n', m] e^{j2\pi m\Delta f(\frac{m'T}{M} - \tau_p)} e^{j2\pi\nu_p(n'T + \frac{m'T}{M})} & \text{if } m' > \frac{M\tau_p}{T}, \\ \sum_{p=1}^P h_p \sum_{m=0}^{M-1} x[n' - 1, m] e^{j2\pi m\Delta f(\frac{m'T}{M} - \tau_p)} e^{j2\pi\nu_p(n'T + \frac{m'T}{M})} & \text{if } m' < \frac{M\tau_p}{T} \end{cases} \end{aligned} \quad (5)$$

applying the DFT and using the orthogonal property, the output is given by

$$\begin{aligned} y[n', m'] &= \frac{1}{\sqrt{M}} \sum_{i=0}^{M-1} y'_{n', i} e^{-j2\pi \frac{m'i}{M}} \\ &= \sum_{p=1}^P \sum_{m=0}^{M-1} (\Psi_{n', m'}^{p,1}[m] x[n' - 1, m] + \Psi_{n', m'}^{p,2}[m] x[n', m]) \end{aligned} \quad (6)$$

where

$$\begin{aligned} \Psi_{n', m'}^{p,1}[m] &= \frac{1}{\sqrt{M}} h_p e^{j2\pi(\nu_p n'T - m\Delta f \tau_p)} \sum_{i=0}^{\lceil \frac{M\tau_p}{T} \rceil} e^{j2\pi \frac{(m - m' + \nu_p T)i}{M}} \\ \Psi_{n', m'}^{p,2}[m] &= \frac{1}{\sqrt{M}} h_p e^{j2\pi(\nu_p n'T - m\Delta f \tau_p)} \sum_{i=\lceil \frac{M\tau_p}{T} \rceil}^{M-1} e^{j2\pi \frac{(m - m' + \nu_p T)i}{M}} \end{aligned} \quad (7)$$

notations $\lceil \cdot \rceil$ and $\lfloor \cdot \rfloor$ indicates the ceil and floor operation, respectively. Equation (6) builds the element-wise relationship between the transmitter and the receiver.

B. Point-to-Point CP-OFDM Transmission

A more standard modulation is CP-OFDM where a CP is added before each data symbol to avoid ISI and to admit symbol-by-symbol detection, we show that the input-output relation in this case can be simplified. The symbol duration for CP-OFDM is $T' = T_{cp} + T$, where T_{cp} is the CP duration, and is configured to be larger than the maximum multipath delay. The transmitted OFDM signal in this case should be altered as

$$f(t) = \sum_{m=0}^{M-1} \sum_{n=0}^{N-1} x[n, m] e^{j2\pi(f_c + m\Delta f)(t - nT')} g_{tx}(t - nT' - T_{cp}) \quad (8)$$

still sampling $y'(t)$ every T/M seconds in each OFDM symbol, but discard the CP samples to remove the ISI, we obtain

$$\begin{aligned} y'_{n', m'} &= y'(t)|_{t=n'T' + T_{cp} + m'T/M} \\ &= \sum_{p=1}^P h_p \sum_{m=0}^{M-1} x[n', m] e^{j2\pi\nu_p(n'T' + T_{cp} + \frac{m'T}{M})} e^{j2\pi m\Delta f(\frac{m'T}{M} - \tau_p)} \end{aligned} \quad (9)$$

after discrete Fourier transform, the output is given by

$$\begin{aligned} y[n', m'] &= \frac{1}{\sqrt{M}} \sum_{i=0}^{M-1} y'_{n', i} e^{-j2\pi \frac{m'i}{M}} \\ &= \frac{1}{\sqrt{M}} \sum_{p=1}^P \sum_{m=0}^{M-1} x[n', m] e^{-j2\pi m\Delta f \tau_p} \\ &\quad e^{j2\pi\nu_p(n'T' + T_{cp})} \text{Dir}(m - m' + \nu_p T, M) \\ &= \sum_{p=1}^P \sum_{m=0}^{M-1} \Psi_{n', m'}^p[m] x[n', m] \end{aligned} \quad (10)$$

where

$$\begin{aligned} \Psi_{n', m'}^p[m] &= \frac{1}{\sqrt{M}} h_p e^{-j2\pi m\Delta f \tau_p} e^{j2\pi\nu_p(n'T' + T_{cp})} \text{Dir}(m - m' + \nu_p T, M) \end{aligned} \quad (11)$$

here we simplify the expression by using the Dirichlet kernel function $\text{Dir}(\phi, Z) = \sum_{z=0}^{Z-1} e^{j2\pi\phi \frac{z}{Z}}$, the value of which is equal to Z (or $-Z$ depending if Z is even or odd) when ϕ is a multiple of Z , and is equal to zero for all other integer values of ϕ .

C. Point-to-Point Zak-OTFS Transmission

For point-to-point OTFS transmission using Zak receiver, the transmitter first maps symbols $x[k, l]$ to samples $X[n, m]$,

from the DD domain to the time-frequency domain using inverse symplectic finite Fourier transform (ISFFT) [5]

$$X[n, m] = \frac{1}{\sqrt{NM}} \sum_{k=0}^{N-1} \sum_{l=0}^{M-1} x[k, l] e^{j2\pi(\frac{nk}{N} - \frac{ml}{M})} \quad (12)$$

for $n = 0, \dots, N-1$, $m = 0, \dots, M-1$. Next, the time-frequency modulator converts the samples $X[n, m]$ to a continuous time waveform $s(t)$ using shaping pulse $g_{tx}(t)$, i.e.,

$$f(t) = \sum_{m=0}^{M-1} \sum_{n=0}^{N-1} X[n, m] e^{j2\pi m \Delta f (t-nT)} g_{tx}(t-nT) \quad (13)$$

$$= \frac{1}{\sqrt{NM}} \sum_{k=0}^{N-1} \sum_{l=0}^{M-1} x[k, l] \beta_{k,l}(t)$$

$$\beta_{k,l}(t) = \sum_{m=0}^{M-1} \sum_{n=0}^{N-1} g_{tx}(t-nT) e^{j2\pi \frac{nk}{N}} e^{j2\pi m \Delta f (t-\frac{lT}{M})} \quad (14)$$

where $\beta_{k,l}(t)$ is the time-domain information carrying signal for the (k, l) -th information symbol $x[k, l]$. Similar to OFDM, with the aid of DD spread function $h(\tau, \nu)$, the received signal after go through the wireless channel is given by

$$y(t) = \sum_{p=1}^P h_p f(t - \tau_p) e^{j2\pi \nu_p t}. \quad (15)$$

In the receiver, in order to decode the transmitted data, the signal is transformed to the DD domain via Zak transform. For the complex time-continuous signal $y(t)$, the Zak representation of which can be written as [11]

$$Z_y(\tau, \nu) = \sqrt{T} \sum_{n=-\infty}^{\infty} y(\tau + nT) e^{-j2\pi n \nu T} \quad (16)$$

which relates the DD representation of the signal and its time domain waveform. The received DD domain samples can be obtained directly by sampling the Zak representation of the received time domain signal without going through a time frequency domain transit, i.e.,

$$Y[k', l'] = Z_y(\tau = l'T/M, \nu = k'\Delta f/N) \quad (17)$$

for $k' = 0, 1, \dots, N-1$, $l' = 0, 1, \dots, M-1$. The transmitted DD domain information symbols $x[k, l]$, $k = 0, 1, \dots, N-1$, $l = 0, 1, \dots, M-1$ are decoded from these received DD domain samples.

D. Point-to-Point Two-Steps OTFS Transmission

For point-to-point OTFS transmission based on two-steps conversion method, the received time signal $y(t)$ first passes through a matched filter to computes the cross ambiguity function in the following way

$$Y(t, f) = \int g_{rx}^*(t' - t) y(t') e^{-j2\pi f t'} dt' \quad (18)$$

where $g_{rx}(t)$ denotes the received pulse shaping function. By substituting (15) and reordering terms, we obtain

$$Y(t, f) = \sum_{n'=0}^{N-1} \sum_{m'=0}^{M-1} X[n', m'] \int \int h(\tau, \nu) \int g_{rx}^*(t' - t) g_{tx}(t' - \tau - n'T) e^{j2\pi m' \Delta f (t' - \tau)} e^{j2\pi \nu t'} e^{-j2\pi f t'} dt' d\tau d\nu \quad (19)$$

the output of the matched filter is obtained by sampling $Y(t, f)$ as

$$Y[n, m] = Y(t, f)|_{t=nT, f=m\Delta f} \quad (20)$$

therefore, we obtain

$$Y[n, m] = \sum_{n', m'} \sum_{p=0}^{P-1} h_p A_c((n-n')T - \tau_p, (m-m')\Delta f - \nu_p) e^{j2\pi \nu_p n'T} e^{j2\pi \nu_p \tau_p} e^{-j2\pi m \Delta f \tau_p} X[n', m']. \quad (21)$$

By applying the SFFT, we obtain the DD domain representation of the received signal as

$$\begin{aligned} Y[k', l'] &= \frac{1}{NM} \sum_{n=0}^{N-1} \sum_{m=0}^{M-1} Y[n, m] e^{-j2\pi(\frac{nk'}{N} - \frac{ml'}{M})} \\ &= \sum_{k,l} \sum_{n, m} \sum_{n', m'} \sum_{p=0}^{P-1} \frac{1}{NM} h_p A_c((n-n')T - \tau_p, \\ &\quad (m-m')\Delta f - \nu_p) e^{j2\pi \nu_p n'T} e^{j2\pi \nu_p \tau_p} e^{-j2\pi m \Delta f \tau_p} \\ &\quad e^{j2\pi(\frac{n'k'}{N} - \frac{m'l'}{M})} e^{-j2\pi(\frac{nk'}{N} - \frac{ml'}{M})} x[k, l] \end{aligned} \quad (22)$$

where $A_c(\tau, \nu)$ is the cross ambiguity function of $g_{tx}(t)$ and $g_{rx}(t)$. Since the received signal $r(t)$ is sampled at time intervals $t' = T/M$, we get

$$\begin{aligned} &A_c((n-n')T - \tau_p, (m-m')\Delta f - \nu_p) \\ &= \frac{T}{M} \sum_{i=-\infty}^{\infty} g_{rx}^*\left(i\frac{T}{M} - (n-n')T + \tau_p\right) g_{tx}\left(i\frac{T}{M}\right) \\ &\quad e^{-j2\pi[(m-m')\Delta f - \nu_p] \frac{iT}{M\Delta f}} \end{aligned} \quad (23)$$

therefore, we obtain

$$\begin{aligned} Y[k', l'] &= \sum_{k,l} \frac{x[k, l]}{NM} T \sum_{p=0}^{P-1} h_p e^{j2\pi \nu_p \tau_p} \left\{ \sum_{n, n'} g_{rx}^*\left(l\frac{T}{M} - (n-n')T + \tau_p\right) g_{tx}\left(l\frac{T}{M}\right) \text{Dir}(l' - l - \tau_p M \Delta f, M) \right. \\ &\quad \left. e^{-j2\pi k' \frac{p}{N}} e^{j2\pi \nu_p \frac{l}{M\Delta f}} e^{j2\pi(k+\nu_p NT) \frac{p}{N}} \right\}. \end{aligned} \quad (24)$$

Consider the default rectangular waveform of $g_{tx}(t)$, and reasonably assume that the maximum possible delay satisfies $\tau < T$, means only the signal of the first preceding symbol duration is involved in the ISI calculation, then the sum $\sum_{n'}$ takes into account only two terms, i.e., $n' = n$ and $n' = n-1$. The indice l involved in the two terms is different since it considers the pulses overlap within the interval $\mathcal{I}_1 = [0, M-1 - \lceil \tau_p M/T \rceil]$ and $\mathcal{I}_2 = [M-1 - \lfloor \tau_p M/T \rfloor, M-1]$. After some algebra we can finally obtain

$$y[k', l'] = \sum_{k=0}^{N-1} \sum_{l=0}^{M-1} \sum_{p=1}^P \Psi_{k',k}^p[l', l] x[k, l] \quad (25)$$

where

$$\begin{aligned} \Psi_{k',k}^p[l', l] &= h_p \frac{1}{MN} e^{j2\pi \nu_p \tau_p} \text{Dir}(\nu_p NT - k' + k, N) \text{Dir}(l' - \\ &\quad l - \tau_p M \Delta f, M) e^{j2\pi \nu_p \frac{l}{M\Delta f}} \begin{cases} 1 & \text{if } l \in \mathcal{I}_1, \\ e^{-j2\pi(\nu_p T + \frac{k}{N})} & \text{if } l \in \mathcal{I}_2. \end{cases} \end{aligned} \quad (26)$$

Reasonably assuming that the maximum possible delay satisfies $\tau < T$, that means only the signal of the first preceding symbol is involved in the ISI calculation. Then the sum $\sum_{n'}$ takes into account only two terms, i.e., $n' = n$ in case that l' residues within the interval $\mathcal{I}'_1 = [\lceil \tau_p M/T \rceil, M-1]$ and $n' = n+1$ in case that l belongs to interval $\mathcal{I}'_2 = [0, \lfloor \tau_p M/T \rfloor]$. We further obtain the channel coefficient as (40) (shown on the top of the next page), where the expression is simplified by using the Dirichlet kernel function $\text{Dir}(\phi, Z) = \sum_{z=0}^{Z-1} e^{j2\pi\phi\frac{z}{Z}}$, the value of which is equal to Z (or $-Z$ depending if Z is even or odd) when ϕ is a multiple of Z , and is equal to zero for all other integer values of ϕ .

Likewise, the signal model of OTFS can also be expressed in matrix form. Although formally the same as the previous OFDM model, it is worth noting that the input-output relationship of the OFDM system is in the time-frequency domain, while for OTFS it is in the DD domain, and the channel matrix Ψ^p should be altered as

$$\Psi^p = \begin{bmatrix} \Psi_{0,0}^p & \cdots & \Psi_{0,N-1}^p \\ \vdots & \ddots & \vdots \\ \Psi_{N-1,0}^p & \cdots & \Psi_{N-1,N-1}^p \end{bmatrix} \quad (41)$$

$$\Psi_{k',k}^p = \begin{bmatrix} \Psi_{k',k}^p[0,0] & \cdots & \Psi_{k',k}^p[0,M-1] \\ \vdots & \ddots & \vdots \\ \Psi_{k',k}^p[M-1,0] & \cdots & \Psi_{k',k}^p[M-1,M-1] \end{bmatrix} \quad (42)$$

For Zak-OTFS, the partial derivatives of $\Psi_{k',k}^p[l',l]$ w.r.t τ_p and ν_p can be obtained as (51) and (52), respectively.

D. CRLB of Two-Steps OTFS

Whereas for OTFS modulation based on the two-step conversion, the derivatives of $\Psi_{k',k}^p[l',l]$ in (26) w.r.t τ_p and ν_p can be obtained as

$$\frac{\partial \Psi_{k',k}^p[l',l]}{\partial \tau_p} = \frac{j2\pi}{NM} h_p \text{Dir}(\nu_p NT - k' + k, N) e^{j2\pi\nu_p(\tau_p + \frac{l}{M\Delta f})} \sum_{m=0}^{M-1} (\nu_p - m\Delta f) e^{j2\pi(l'-l-\tau_p M\Delta f)\frac{m}{M}} \begin{cases} 1 & \text{if } l \in \mathcal{I}_1, \\ e^{-j2\pi(\nu_p T + \frac{k}{N})} & \text{if } l \in \mathcal{I}_2, \end{cases} \quad (43)$$

$$\frac{\partial \Psi_{k',k}^p[l',l]}{\partial \nu_p} = \frac{j2\pi}{NM} h_p \text{Dir}(l' - l - \tau_p M\Delta f, M) e^{j2\pi\nu_p(\tau_p + \frac{l}{M\Delta f})} \sum_n e^{j2\pi(\nu_p NT - k' + k)\frac{n}{N}} \begin{cases} \frac{l}{M\Delta f} + nT + \tau_p & \text{if } l \in \mathcal{I}_1, \\ (\frac{l}{M\Delta f} + nT + \tau_p - T) e^{-j2\pi(\nu_p T + \frac{k}{N})} & \text{if } l \in \mathcal{I}_2. \end{cases} \quad (44)$$

The CRLB of time delays and Doppler shifts follows by filling the Fisher information matrix (FIM) with the derivatives deduced above. FIM is defined as [8]

$$\mathbf{J}(\boldsymbol{\theta}) = \mathbb{E} \left\{ \left[\frac{\partial}{\partial \boldsymbol{\theta}} \log p(\mathbf{y}, \boldsymbol{\theta}) \right] \left[\frac{\partial}{\partial \boldsymbol{\theta}} \log p(\mathbf{y}, \boldsymbol{\theta}) \right]^T \right\} \quad (45)$$

where the vector $\boldsymbol{\theta} \in \mathbb{R}^{4P}$ consists of all parameters of the P paths. Specifically, for path p , it includes τ_p and ν_p , as well as the amplitude and phase of h_p . $p(\mathbf{y}, \boldsymbol{\theta})$ is the likelihood function of \mathbf{y} when $\boldsymbol{\theta}$ is observed. Assume that the received signal is interfered by an additive white Gaussian noise $\mathbf{n} \sim$

$\mathcal{CN}(\mathbf{0}, \boldsymbol{\Sigma})$, where $\boldsymbol{\Sigma}$ is the covariance matrix, therefore we have $\mathbf{y} \sim \mathcal{CN}(\boldsymbol{\Psi}\mathbf{x}, \boldsymbol{\Sigma})$. It can be obtained that the logarithm probability function of \mathbf{y} w.r.t $\boldsymbol{\theta}$ is

$$\Lambda = \log p(\mathbf{y}, \boldsymbol{\theta}) = -(\mathbf{y} - \boldsymbol{\Psi}\mathbf{x})^H \boldsymbol{\Sigma}^{-1} (\mathbf{y} - \boldsymbol{\Psi}\mathbf{x}) - C \quad (46)$$

where C is a constant term that is not concerned. Based on (46) we have

$$\frac{\partial \Lambda}{\partial \theta_i} = -(\mathbf{y} - \boldsymbol{\Psi}\mathbf{x})^H \boldsymbol{\Sigma}^{-1} \frac{\partial \boldsymbol{\Psi}}{\partial \theta_i} \mathbf{x} - \left(\frac{\partial \boldsymbol{\Psi}}{\partial \theta_i} \mathbf{x} \right)^H \boldsymbol{\Sigma}^{-1} (\mathbf{y} - \boldsymbol{\Psi}\mathbf{x}) \quad (47)$$

since $\mathbb{E}\{\mathbf{y} - \boldsymbol{\Psi}\mathbf{x}\} = 0$, it can be got that $\mathbb{E}\{\frac{\partial \Lambda}{\partial \theta_i}\} = 0, \forall i$. Therefore, we can obtain

$$\mathbb{E} \left\{ \frac{\partial^2 \Lambda}{\partial \theta_i \partial \theta_j^*} \right\} = -2\Re \left\{ \left(\frac{\partial \boldsymbol{\Psi}}{\partial \theta_j} \mathbf{x} \right)^H \boldsymbol{\Sigma}^{-1} \frac{\partial \boldsymbol{\Psi}}{\partial \theta_i} \mathbf{x} \right\} \quad (48)$$

hence the FIM $\mathbf{J}(\boldsymbol{\theta})$ can be obtained as

$$\begin{cases} \mathbf{J}(\boldsymbol{\theta}) = [J_{i,j}]_{1 \leq i,j \leq 4P} \\ J_{i,j} = -\mathbb{E} \left(\frac{\partial^2 f}{\partial \theta_i \partial \theta_j^*} \right) \end{cases} \quad (49)$$

the MSE of any unbiased estimator $\hat{\boldsymbol{\theta}}$ satisfies

$$\mathbb{E}\{(\hat{\boldsymbol{\theta}} - \boldsymbol{\theta})(\hat{\boldsymbol{\theta}} - \boldsymbol{\theta})^T\} \succeq \mathbf{J}^{-1}(\boldsymbol{\theta}) \quad (50)$$

where the main diagonal elements of $\mathbf{J}^{-1}(\boldsymbol{\theta})$ are the desired CRLBs for the unknown parameters.

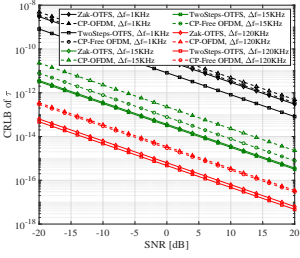
IV. NUMERICAL RESULTS

In this section, we evaluate the CRLB of OFDM and OTFS modulations as functions of signal-to-noise ratio (SNR), SCS, as well as PRB size. Firstly, we consider a single path, SCS= 15KHz, and fix the PRB size to be $M = N = 12$. The CRLB of delay and Doppler shift versus SNR is presented in Fig. 1, which shows that the bound of delay estimation decreases with increasing SCS, and vice versa for that of Doppler shift, because a large SCS implies a wide bandwidth and short time duration. This reveals that it is feasible to satisfy the sensing requirements of various applications by adjusting the SCS. Next, Fig. 2 shows the impact of PRB size on the CRLB. As expected, more PRBs help improve sensing accuracy, which is still essentially a result of changes in bandwidth and time duration in the case of a given SCS. Besides, given PRB size, diverse delay and Doppler estimation performance can be met by tuning M and N combinations. Finally, we present the CRLBs of τ 's and ν 's in the multipath case in Fig. 3, where the first path has lower delay and Doppler CRLB than the second path due to higher signal strength. Overall, OTFS has a dominant advantage in delay and Doppler estimation compared to OFDM, where the Zak-OTFS and the Two-Steps OTFS outperform other schemes in terms of delay and Doppler shift estimation, respectively. The bound for CP-Free OFDM or CP-OFDM are comparable.

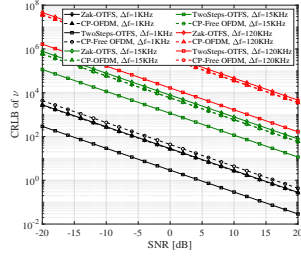
$$\Psi_{k',k}^p[l',l] = \begin{cases} \frac{1}{\sqrt{MN}} h_p e^{j2\pi\nu_p \frac{l'T}{M}} \text{Dir}(l' - l - \tau_p \Delta f M, M) \text{Dir}(k - k' + \nu_p T N, N) & \text{if } l' \in \mathcal{I}'_1, \\ \frac{1}{\sqrt{MN}} h_p e^{j2\pi\nu_p \frac{l'T}{M}} e^{j2\pi\nu_p T} e^{-j2\pi \frac{k'}{N}} \text{Dir}(l' - l - \tau_p \Delta f M, M) \text{Dir}(k - k' + \nu_p T N, N) & \text{if } l' \in \mathcal{I}'_2 \end{cases} \quad (40)$$

$$\frac{\partial \Psi_{k',k}^p[l',l]}{\partial \tau_p} = \begin{cases} \frac{1}{\sqrt{MN}} h_p e^{j2\pi\nu_p \frac{l'T}{M}} \text{Dir}(k - k' + \nu_p T N, N) \sum_{m=0}^{M-1} [-j2\pi m \Delta f] e^{j2\pi m \frac{l'-l}{M}} e^{j2\pi m \Delta f \tau_p} & \text{if } l' \in \mathcal{I}'_1, \\ \frac{1}{\sqrt{MN}} h_p e^{j2\pi\nu_p \frac{l'T}{M}} e^{j2\pi\nu_p T} e^{-j2\pi \frac{k'}{N}} \text{Dir}(k - k' + \nu_p T N, N) \sum_{m=0}^{M-1} [-j2\pi m \Delta f] e^{j2\pi m \frac{l'-l}{M}} e^{j2\pi m \Delta f \tau_p} & \text{if } l' \in \mathcal{I}'_2 \end{cases} \quad (51)$$

$$\frac{\partial \Psi_{k',k}^p[l',l]}{\partial \nu_p} = \begin{cases} \frac{1}{\sqrt{MN}} h_p \text{Dir}(l' - l - \tau_p \Delta f M, M) \sum_{n=0}^{N-1} [j2\pi(\frac{l'T}{M} + nT)] e^{j2\pi n \frac{(k-k')}{N}} e^{j2\pi(\frac{l'T}{M} + nT)\nu_p} & \text{if } l' \in \mathcal{I}'_1, \\ \frac{1}{\sqrt{MN}} h_p e^{-j2\pi \frac{k'}{N}} \text{Dir}(l' - l - \tau_p \Delta f M, M) \sum_{n=0}^{N-1} [j2\pi(\frac{l'T}{M} + nT + T)] e^{j2\pi n \frac{(k-k')}{N}} e^{j2\pi(\frac{l'T}{M} + nT + T)\nu_p} & \text{if } l' \in \mathcal{I}'_2 \end{cases} \quad (52)$$

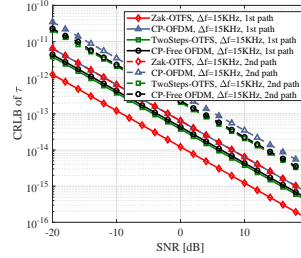


(a) CRLB of delay versus SNR

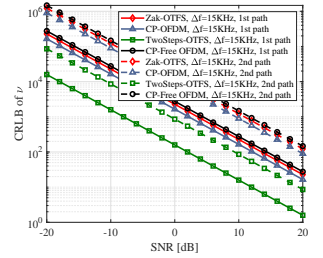


(b) CRLB of Doppler versus SNR

Fig. 1. CRLB illustration of τ and ν versus SNR. Key configurations includes $N = M = 12$, $f_c = 3\text{GHz}$, $\tau = 3.33 \times 10^{-6}\text{s}$ and $\nu = 500\text{Hz}$.

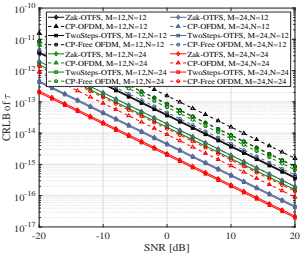


(a) CRLB of delay versus SNR

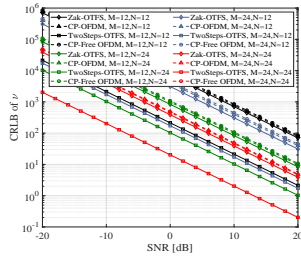


(b) CRLB of Doppler versus SNR

Fig. 3. CRLB illustration of τ and ν versus SNR in case of two paths channel. Key parameters includes $M = N = 12$, $h_1 = 0.7e^{j\pi/3}$, $h_2 = 0.3e^{j3\pi/4}$, $\tau_1 = 3.33 \times 10^{-6}\text{s}$, $\nu_1 = 500\text{Hz}$, $\tau_2 = 5 \times 10^{-6}\text{s}$ and $\nu_2 = 2.5\text{KHz}$.



(a) CRLB of delay versus MN



(b) CRLB of Doppler versus MN

Fig. 2. CRLB illustration of τ and ν versus the size of M and N . Other parameters are the same as Fig. 1.

V. CONCLUSION

In this paper, we investigated the sensing performance of OTFS and OFDM modulation systems based on the constructed point-to-point transmission models. For OFDM, we consider the ideal CP-Free and the practical CP-added models, respectively, while for OTFS, both the Zak transform based and the Two-Step conversion based receivers are considered. The CRLBs for the delay and Doppler shift under these four models are then derived, respectively. Numerical results validate that OTFS outperforms OFDM for sensing, while the Zak-OTFS and the Two-Steps OTFS outperform other schemes in terms of delay and Doppler shift estimation, respectively. In addition, the analysis of the effect of SCS and PRB size on the CRLB provides guidance on satisfying the sensing requirements of various scenarios through flexible parameter tuning.

REFERENCES

- [1] A. Liu, Z. Huang, M. Li, Y. Wan, W. Li, T. X. Han, C. Liu, R. Du, D. K. P. Tan, J. Lu, Y. Shen, F. Colone, and K. Chetty, "A survey on fundamental limits of integrated sensing and communication," *IEEE Communications Surveys & Tutorials*, vol. 24, no. 2, pp. 994–1034, 2022.
- [2] G. Stuber, J. Barry, S. McLaughlin, Y. Li, M. Ingram, and T. Pratt, "Broadband MIMO-OFDM wireless communications," *Proceedings of the IEEE*, vol. 92, no. 2, pp. 271–294, 2004.
- [3] T. Wang, Y. Shen, S. Mazuelas, H. Shin, and M. Z. Win, "On OFDM ranging accuracy in multipath channels," *IEEE Systems Journal*, vol. 8, no. 1, pp. 104–114, 2014.
- [4] C. Sturm and W. Wiesbeck, "Waveform design and signal processing aspects for fusion of wireless communications and Radar sensing," *Proceedings of the IEEE*, vol. 99, no. 7, pp. 1236–1259, 2011.
- [5] P. Raviteja, K. T. Phan, Y. Hong, and E. Viterbo, "Interference cancellation and iterative detection for orthogonal time frequency space modulation," *IEEE Transactions on Wireless Communications*, vol. 17, no. 10, pp. 6501–6515, 2018.
- [6] L. Gaudio, M. Kobayashi, G. Caire, and G. Colavolpe, "On the effectiveness of OTFS for joint Radar parameter estimation and communication," *IEEE Transactions on Wireless Communications*, vol. 19, no. 9, pp. 5951–5965, 2020.
- [7] P. Raviteja, K. T. Phan, Y. Hong, and E. Viterbo, "Orthogonal time frequency space (OTFS) modulation based Radar system," in *2019 IEEE Radar Conference (RadarConf)*, 2019, pp. 1–6.
- [8] S. K. Sengupta, "Fundamentals of statistical signal processing: Estimation theory," *Technometrics*, vol. 37, no. 4, pp. 465–466, 1993.
- [9] S. K. Mohammed, "Derivation of ofts modulation from first principles," *IEEE Transactions on Vehicular Technology*, vol. 70, no. 8, pp. 7619–7636, Mar. 2021.
- [10] P. Bello, "Characterization of randomly time-variant linear channels," *IEEE Transactions on Communications Systems*, vol. 11, no. 4, pp. 360–393, 1963.
- [11] A. J. Janssen, "The Zak transform: a signal transform for sampled time-continuous signals," *Philips Journal of Research*, vol. 43, no. 1, pp. 23–69, 1988.